Integration of multiple signaling pathway activities resolves K-RAS/N-RAS mutation paradox in colon epithelial cell response to inflammatory cytokine stimulation

Integration of multiple signaling pathway activities resolves K-RAS/N-RAS mutation paradox in colon epithelial cell response to inflammatory cytokine stimulation†

Pamela K. Kreeger,‡*[a] Yufang Wang,[bc] Kevin M. Haigis[bc] and Douglas A. Lauffenburger*[ad]

Received 9th December 2009, Accepted 1st February 2010
First published as an Advance Article on the web 8th March 2010
DOI: 10.1039/b925935j

Colon tumors frequently harbor mutation in K-RAS and/or N-RAS, members of a GTPase family operating as a central hub for multiple key signaling pathways. While these proteins are strongly homologous, they exhibit diverse downstream effects on cell behavior. Utilizing an isogenic panel of human colon carcinoma cells bearing oncogenic mutations in K-RAS and/or N-RAS, we observed that K-RAS and double mutants similarly yield elevated apoptosis in response to treatment with TNFα compared to N-RAS mutants. Regardless, and in surprising contrast, key phospho-protein signals were more similar between N-RAS and dual mutants. This apparent contradiction could not be explained by any of the key signals individually, but a multi-pathway model constructed from the single-mutant cell line data was able to predict the behavior of the dual-mutant cell line. This success arises from a quantitative integration of multiple pro-apoptotic (pIκBα, pERK2) and pro-survival (pJNK, pHSP27) signals in manner not easily discerned from intuitive inspection.

Introduction

Upon activation by receptor tyrosine kinases, the RAS family of GTPases (K-RAS4A, K-RAS4B, H-RAS, and N-RAS) signal to multiple downstream effector pathways. Single amino acid mutations at codons 12, 13, or 61 place RAS in a chronically active (GTP-bound) state and are oncogenic.[1] While K-RAS and N-RAS are greater than 90% homologous and share many of the same downstream effectors,[2] several lines of evidence indicate that the RAS isoforms have distinct physiological functions. For example, mouse models of K-Ras^{G12D} and N-Ras^{G12D} expressed in the colonic epithelium show distinct phenotypes, with K-Ras^{G12D} stimulating hyper-proliferation and N-Ras^{G12D} conferring resistance to apoptosis.[3] Oncogenic K-RAS promotes butyrate-induced apoptosis in human colon carcinoma cells[4] while N-RAS provides anti-apoptotic signals in mouse embryonic fibroblasts,[5] indicating that apoptosis is a key cellular process that is differentially regulated by the RAS family members.

Historical data for colon cancer suggest that mutations in K-RAS and N-RAS can co-exist in an individual tumor,[6] raising the question of why a given tumor might select for two mutations that exert opposite effects on a key oncogenic process such as apoptosis. To help address this question, we examine here the impact of simultaneous mutation of both N-RAS and K-RAS on the response of colon carcinoma cells to exposure to the inflammatory cytokine tumor necrosis factor-α (TNFα), which is appreciated to be intimately

[a] *Department of Biological Engineering, Massachusetts Institute of Technology, 77 Massachusetts Ave, 16-343, Cambridge, MA 02139, USA. Tel: +1 (617) 252-1629*
[b] *Molecular Pathology Unit and Center for Cancer Research, Massachusetts General Hospital, Charlestown, MA 02129, USA*
[c] *Department of Pathology, Harvard Medical School, Boston, MA 02115, USA*
[d] *Center for Cancer Research, Massachusetts Institute of Technology, Cambridge, MA 02139, USA. E-mail: lauffen@mit.edu*
† **Financial support:** This work was funded by National Institutes of Health Grants U54-CA112967 and P50-GM68762, and by the American Cancer Society (PF-08-026-01-CCG to P.K.K).
‡ Current contact: University of Wisconsin-Madison, Department of Biomedical Engineering.

Insight, innovation, integration

Activating mutations in the RAS GTPases have been identified in over 30% of all cancers; however, the impact of these mutations on the cellular signaling network and phenotypic behavior is generally confusing. Here, we utilize a novel systems biology approach that integrates experimental and computational techniques to analyze the impact of activating mutations in K-RAS, N-RAS, either alone or in combination, in human colon epithelial cells on the response to the inflammatory cytokine TNFα. Through our analysis, we have identified an important quantitative balance between multiple pro-survival *versus* pro-apoptotic pathways that resolves seemingly contradictory behavior of dual RAS mutant cells relative to cells with either individual mutation.

involved in tumor progression in the colon as well as in other tissues.[7] We observe that the dual-mutant cells phenocopy K-RAS single mutant cells with respect to their apoptotic response to TNFα even while signaling patterns for key pathways in the dual mutants are more similar to those in N-RAS mutant cells. To resolve this paradox, we construct a multi-pathway partial least squares regression (PLSR) model from the single mutant cell data and test its ability to predict the sensitivity of the dual-mutant cells. We find that this model successfully predicts the extent of apoptosis for the dual-mutant condition, on the basis of a quantitative balance between multiple pro-apoptotic signals (pERK2, pIκBα) and pro-survival signals (pJNK, pHSP27). The capability of this single model to comprehend cellular information processing with respect to cytokine-challenged survival, invariantly across the different RAS mutation genotypes, implies that the cells could transition relatively seamlessly from one mutation to another (or have both co-exist) during dynamic changes in degree of inflammatory context that might in some cases be problematic for the K-RAS mutation.[8]

Materials and methods

Cell lines and treatments

DLD-1, a colon carcinoma cell line with a single copy K-RAS^{G13D} mutation, and DKs8-N, which over-express mutant N-RAS^{G12V} in an isogenic wild-type K-RAS background, have previously been described.[9,10] DLD-N were generated by infecting DLD-1 cells with pBabe retrovirus carrying N-Ras^{G12D}. All cell lines were maintained in DMEM supplemented with 10% fetal bovine serum (FBS). For experiments, cells were plated in 10% FBS at 15 000 cells cm^{-2}; after 24 h, cells were sensitized with 200 units mL^{-1} interferon-γ (IFNγ, Roche Applied Science, Indianapolis, IN) in 5% FBS. After 24 h, cells were treated with either vehicle or 100 ng mL^{-1} TNFα (Peprotech, Rocky Hill, NJ). Data are represented as average ±SEM for three biological replicates.

RAS characterization

The levels of active K- and N-RAS were assessed with a RAS activation assay kit (Upstate, Billerica, MA). Briefly, cells were washed twice with ice-cold PBS and then lysed with MLB buffer (25 mM HEPES, pH 7.5, 150 mM NaCl, 1% Igepal CA-630, 10 mM $MgCl_2$, 1 mM EDTA and 2% glycerol) containing protease and phosphatase inhibitors (Roche Applied Science). After centrifugation at 14 000 × g for 5 min, protein levels were quantified using the Bio-Rad Protein Assay Kit (Bio-Rad Laboratories, Hercules, CA). Cell lysates containing 1 mg of protein were incubated at 4 °C for 120 min with 10 μL of agarose bound with glutathione S-transferase fusion protein corresponding to the human RAS-binding domain (RBD, residues 1–149) of RAF1. After the samples were washed three times with MLB, active RAS was eluted and the levels of active K- and N-RAS were determined by Western blotting analysis. Membranes were blocked with Odyssey Blocking Buffer (Li-Cor, Lincoln, NE), probed with anti-*N*-RAS (sc-31) or anti-K-RAS (sc-30, Santa Cruz, Biotechnology, Santa Cruz, CA), detected with Donkey-anti-mouse-800, and imaged on the Odyssey infrared imaging system (Li-Cor). 30 μg of cell lysate was also analyzed for total levels of K- and N-RAS with the same antibodies and anti-tubulin (Sigma, St. Louis, MO).

Lysis and signaling measurements

At various times after TNFα stimulation (0, 5, 15, 30, 60, 90, 120, 240, 480, and 720 min) cells were lysed using Bio-Plex cell lysis buffer (Bio-Rad). Total protein concentrations were determined using the bicinchoninic acid assay (Pierce, Rockford, IL). The levels of four phospho-proteins (pERK2, pIκBα, pJNK, and pHSP27) were detected using commercially available kits for the Luminex system (Bio-Rad). These proteins were chosen as they are in the 'middle layer' of several key signal transduction pathways and were informative in our prior studies.[11] pHSP27 was chosen as a readout of p38, which did not provide a robust signal by this method in our preliminary studies (data not shown). A master positive-reference sample was loaded in each assay for normalization purposes. Full time courses were performed once for each condition with three biological replicates and technical duplicates. Median CV's were 10.8% (technical duplicates) and 18.7% (biological replicates). A subset of timepoints were independently repeated to determine overall variation,[12] with a media CV of 16.9%, indicating that assay, biological, and day-to-day variation are of similar magnitude and the data set is self-consistent. Importantly, in the repeated samples, trends within and between samples were preserved. Data is represented as average ±SEM. Hierarchical clustering analysis on the resulting data set was performed in Spotfire (TIBCO, Palo Alto, CA) with the unweighted pair group method using arithmetic averages (UPGMA) and Euclidean distances. The integrated level of each signal was determined by trapezoid rule.[13]

Flow cytometry

Floating and adherent cells were pooled and analyzed for apoptosis using cleaved caspase-3/cleaved PARP similar to the previously described methods.[12] Cells were fixed with 4% paraformaldehyde, permeabilized with Tween, and stained using anti-cleaved caspase-3 (1 : 500) and anti-cleaved PARP (1 : 250, BD Pharmingen, Franklin Lakes, NJ), followed by Alexa 488-donkey-anti-rabbit IgG and Alexa 647-donkey-anti-mouse IgG (both at 1 : 250, Invitrogen, Carlsbad, CA). A minimum of 25 000 cells per condition was analyzed on a BD Biosciences LSRII (part of the Koch Institute Flow Cytometry Core Facility, MIT) and by FlowJo (Tree Star, Inc, Ashland, OR).

Partial least squares regression (PLSR) modeling

Multi-pathway models were generated using the PLSR algorithm in SimcaP (Umetrics, Kinnelon, NJ—see ref. 14 for details). Briefly, an independent block matrix (**X**, dimensions *MxN*) was generated with each column corresponding to the data for a single time point and phosphoprotein. There were 40 columns in total (10 times × 4 phosphoproteins). Each row represented a different cellular condition, with a

total of four rows corresponding to untreated and TNFα treated DLD-1 and DKs8-N cells. A dependent matrix (**Y**, dimensions *MxP*) was generated from the cellular output data, with the rows corresponding to the same cellular conditions listed above and three columns for the level of apoptosis at each time. All data were mean-centered and unit variance scaled. PLSR was used to solve the regression problem:

$$Y = Xb + e \quad (1)$$

where **b** is the vector containing the regression coefficients and **e** is the residual. A nonlinear iterative partial least squares (NIPALS) algorithm was used.[15] It is instructive to note that the NIPALS algorithm applied to a single *MxN* matrix (**X**) is the representation of the matrix as a sum of outer products such that:

$$X = t_1p_1' + t_2p_2' + \cdots + e \quad (2)$$

where t_i is called the scores vector and represents one dimension in the orthogonal basis set for the column space and p_i is called the loadings vector and represents one dimension in the orthogonal basis set for the row space. The NIPALS algorithm was implemented as described elsewhere.[16] Briefly, an iterative process is used to define two vectors, *w* and *c*, that maximize the following term:

$$[\mathrm{Cov}(t,u)]^2 = [\mathrm{Cov}(Xw,Yc)]^2 \quad (3)$$

where *t* and *u* are the scores vectors for the **X** and **Y** matrices, respectively. Loadings vectors for **X** and **Y**, called *p* and *q*, respectively, are also defined as:

$$p = X^Tt/(t^Tt);\ q = Y^Tu/(u^Tu) \quad (4)$$

The set of vectors *t*,*u*,*w*, and *c* are associated with the maximum eigenvalues for various covariance matrices, and once defined, their contribution is removed from the **X** and **Y** matrices, leaving a residual matrix that can be further modeled with a new set of *t*,*u*,*w*,*c*,*p*, and *q* vectors. Each model was tested for goodness of prediction (Q^2) using a leave-one-out cross validation approach.[16] Briefly, cross-validation was performed by omitting an observation from the model development and then using the model to predict the **Y**-matrix values for the withheld observation. This procedure was repeated until every observation has been kept out exactly once. To predict the novel DLD-N condition and analyze the impact of individual phosphoprotein timecourses, the resulting **Y** matrix for each new **X** signaling matrix was determined by the derived PLSR function.

Results

To explore the impact of single *versus* dual mutations in RAS, we utilized a panel of isogenic colon carcinoma cell lines with either a mutant form of K-RAS (DLD-1), mutant N-RAS (DKs8-N), or both mutations (DLD-N, depicted in Fig. 1A). Western blot analysis confirmed the elevation in active K-RAS in DLD-1 and DLD-N and active N-RAS in DLD-N and DKs8-N (Fig. 1B). As expected, there is an increase in total N-RAS levels with the over-expression of active N-RAS. Interestingly, N-RAS over-expression also results in a slight

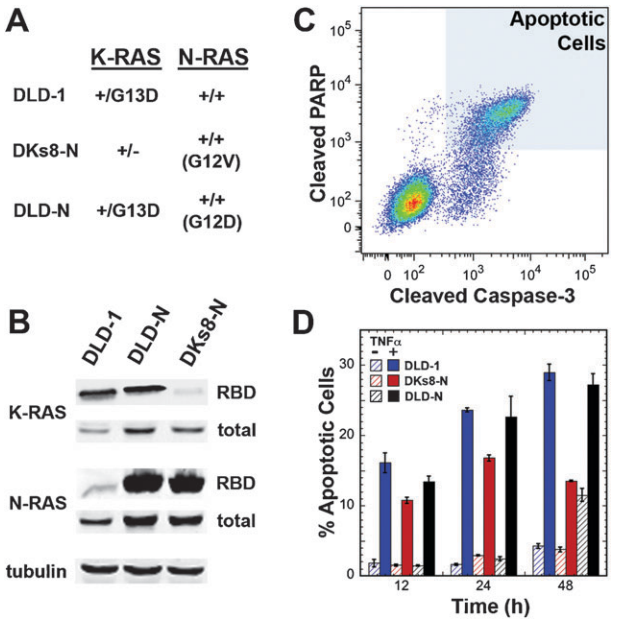

Fig. 1 Cells with mutations in both N-RAS and K-RAS are sensitive to TNFα. **(A)** Overview of the *RAS* genotypes of the three cell lines. **(B)** Levels of active (RBD) and total K- and N-RAS for each cell line. **(C)** The percentage of apoptotic cells was determined by flow cytometry from the percentage of cells that were positive for both cleaved caspase-3 and cleaved PARP. **(D)** DLD-1 and DLD-N cells demonstrated a similar sensitivity to TNFα, while DKs8-N cells were more resistant.

increase in total K-RAS, preserving the ratio of N-RAS to K-RAS. TNFα treatment of this panel of cell lines results in a significant increase in apoptosis as measured by positive staining for cleaved caspase-3 and cleaved PARP (Fig. 1C). We have previously demonstrated that DLD-1 cells were more sensitive to TNFα treatment than DKs8-N;[11] here, we observed that DLD-N cells were as sensitive to TNFα as DLD-1 cells (Fig. 1D). Forty-eight hours after TNFα treatment, 27% of DLD-N cells and 29% of DLD-1 cells stained positive for cleaved caspase-3/cleaved PARP, while only 14% of DKs8-N cells were apoptotic. Thus, the effect of having both K-RAS and N-RAS mutated on TNFα-induced cell death is to yield essentially the same apoptosis-sensitization as the K-RAS mutation by itself. In essence, mutant K-RAS is epistatic to mutant N-RAS with respect to TNFα-induced apoptosis.

Previously, we examined the dynamics of several phosphorylated proteins across key signaling pathways downstream of TNFα treatment in DLD-1 and DKs8-N cells, and found that these signals were sufficient to predict apoptosis and chemokine levels.[11] Accordingly, we quantified the levels of phosphorylated ERK2, HSP27, IκBα, and JNK in DLD-N cells following TNFα treatment using high-throughput, multiplexed assays and the Luminex platform (Fig. 2A). TNFα treatment led to increased levels of each of the phosphoproteins examined, with dynamics that differed based on the genetic configuration of the cell. For example, DLD-1 cells demonstrated weak activation of pERK2, pJNK, and pHSP27, but robust increases in pIκBα. In contrast, DKs8-N and DLD-N cells showed activation of all proteins.

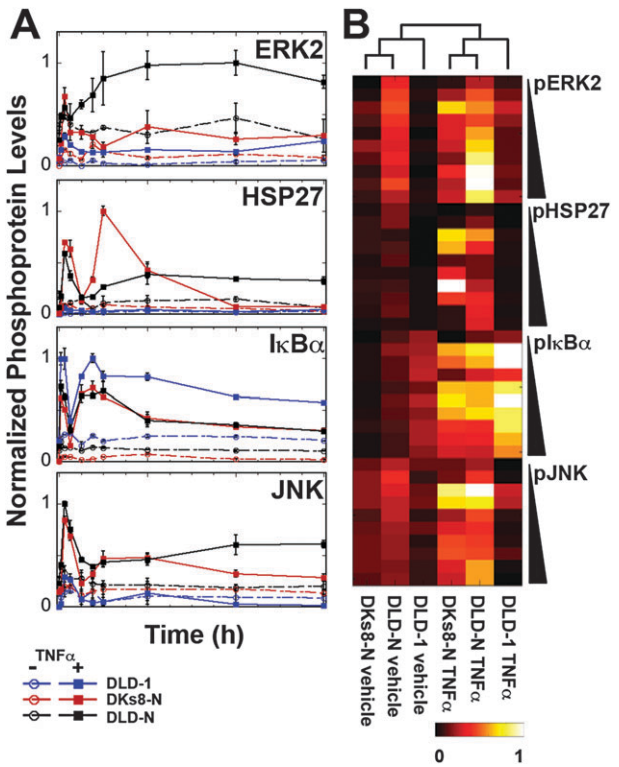

Fig. 2 Signaling dynamics in response to TNFα treatment. **(A)** Individual time courses for the four phosphoproteins indicated that DKs8-N and DLD-N cells had similar signaling dynamics. **(B)** Cluster analysis by UPGMA confirmed the similarity between DKs8-N and DLD-N cells. Each box represents the scaled average signal for a particular time, ordered from early to late times.

The dynamics of pERK2 were strikingly different between DLD-N and DKs8-N or DLD-1 cells, with elevated levels of pERK2 seen for longer time periods. Overall, the pattern of signaling behavior between DKs8-N and DLD-N was similar, and analysis by hierarchical clustering confirmed that DLD-N and DKs8-N clustered separately from DLD-1 within both the untreated and TNFα-treated branches (Fig. 2B). In surprising contrast to the apoptosis results, then, the effect of having both K-RAS and N-RAS mutated on TNFα-induced cell signaling is fairly similar to that of the N-RAS mutation by itself.

Accordingly, we face a paradox: the behavior of double K-/N-RAS mutation in response to TNFα is similar to N-RAS mutation by itself with respect to signaling but is similar to K-RAS mutation by itself with respect to apoptosis. In order to understand how this puzzle might be resolved, we use a systems modeling approach, partial least-square regression (PLSR), previously found to be helpful in ascertaining the most informative combinations of signals for predicting phenotypic behavior.[11] In PLSR, the **X** matrix (phosphoprotein levels) is regressed against the **Y** matrix (apoptosis), and dimensionality is reduced by combining independent measurements that strongly co-vary with the dependent outcomes into principal components.[15] The first principal component captures the strongest variation in the original data matrix, while succeeding principal components capture remaining variation. In our previous studies of various individual mutations, the N-RAS mutation effects and K-RAS mutation effects were clearly distinguishable by their quantitative differences in contribution to the second principle component, while the first principle component mainly characterized the effects of TNFα treatment.

Employing this methodology here, a PLSR model constructed from the signaling and response data for untreated and TNFα treated DLD-1 and Dks8-N cells was found to fit the data well, with an R^2Y of 0.95 and a Q^2Y of 0.75 (Fig. 3A). Previous reports by our group have utilized the integrated signal intensity or time derivatives as metrics within the **X** matrix of the model.[17,18] However, since these metrics are a linear combination of signals, it adds no new information in PLSR, which is a linear model form; rather, it could be used to represent the contribution of individual timepoints in aggregate. Given the small size of the **X** matrix in this new study, we found that the individual data points provide more substantial contributions. Similar to our previous model incorporating wildtype-RAS cells,[11] the projection of the various conditions along the scores of the model demonstrated that the first component was a 'TNFα treatment' axis (Fig. 3B). Confirming this interpretation, signaling data from pERK2 and pIκBα weighed strongly in the first component (Fig. 3C); these signals result from TNFα treatment by virtue of TNFR activation of the NFκB pathway and transactivation of a TGFα autocrine loop.[11,13,19] pHSP27 and pJNK have negative loadings in the second component, in agreement with their activation in DKs8-N cells that have negative scores in the second component.

PLSR models might be generally expected to predict similar phenotypic responses for conditions with similar signaling patterns. In the double RAS mutants, however, we identified similar signaling behavior, but divergent apoptotic response, between DLD-N and DKs8-N cells. Therefore, we might have expected that the PLSR model constructed from single RAS mutant cells would have difficulty predicting the response of double mutant cells. Nonetheless, in a direct test of the model's ability to predict DLD-N apoptosis from the DLD-N signaling data we found successful prediction of elevated sensitivity of the DLD-N double mutants compared to DKs8-N (Fig. 3A).

To understand conceptually how the PLSR model was able to reconcile the apparent contradiction between DLD-N signaling behavior and apoptotic response, we generated a series of modified DLD-N data sets, with three of four phospho-protein time-courses from DLD-N experimental data and the fourth a substitution of either DLD-1 or DKs8-N data. For example, for the pERK2 substitution, pJNK, pHSP27, and pIkBα data would all be used from the DLD-N cells, while pERK2 time courses would be substituted from either the DLD-1 or DKs8-N cells. Using these mixed data sets, apoptosis was predicted from the PLSR model (Fig. 4A); in this way, we could modify the characteristics of each set of phospho-proteins to parse its contribution. For example, DLD-N has elevated pERK2 relative to both cell lines (Fig. 2A) and pERK2 contributes positively to apoptosis (component 1, Fig. 3C). Correspondingly, substitution of either DLD-1 or DKs8-N pERK2 signaling into the DLD-N data set resulted in a prediction of apoptosis that was lower

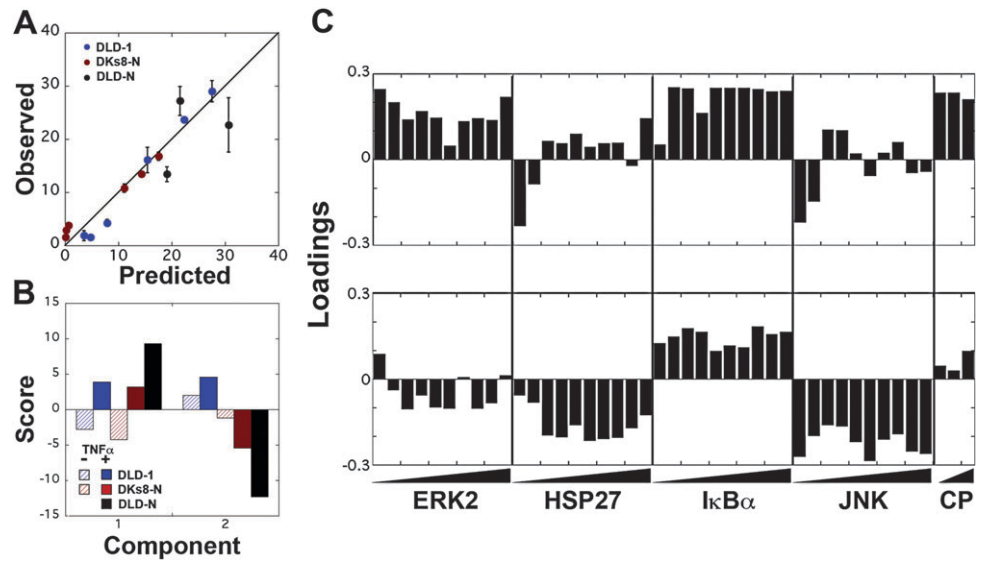

Fig. 3 A PLSR model built on single-mutant signaling and apoptosis is able to predict dual-mutant apoptosis. **(A)** The PLSR model accurately predicted the elevated sensitivity of DLD-N cells to TNFα. **(B)** Scores for the three cell lines in the first and second component. The first component is consistent with a 'TNFα treatment' axis. **(C)** Loadings for the first two components of the single-mutant PLSR model. CP indicates the loadings for the response metric of cleaved caspase-3 and cleaved PARP positive cells.

than the intact DLD-N data set (Fig. 4A). Similarly, DLD-N cells have lower pIκBα than DLD-1 cells; when a prediction was made with DLD-1 levels of pIκBα, apoptosis increased as would be expected from the heavy positive loading of pIκBα for apoptosis. Substitution of the elevated pERK2 or lower pIκBα levels from DLD-N to the DLD-1 data set also increased the predicted apoptosis (data not shown). In the second component of the model (Fig. 3C), pJNK contributed negatively to apoptosis; as DLD-N have elevated pJNK relative to both of the single mutant cell lines (Fig. 2A), the decrease in pJNK with the single mutant substitution resulted in a small increase in apoptosis (Fig. 4A). pHSP27 does not contribute as strongly or consistently in the model loadings and substitution of pHSP27 had only a slight impact on the predicted level of apoptosis. To quantitatively determine the impact of each signaling change, we calculated the integrated level for each signal's timecourse and determined the difference between the DLD-N integrated level and the integrated level from the substitute data (Table 1). Comparing the differences between DLD-N and mixed data set apoptosis predictions, and the change in each integrated signal, we were able to identify the model interpretation for each signal (Fig. 4B). pIκBα and pERK2 are both pro-apoptotic while pJNK and pHSP27 are pro-survival influences. We conclude that the PLSR model predominantly monitors the combined contributions from pERK2 and pIκBα with counteracting combined contributions from pJNK and pHSP27. Hence, in DLD-N

Table 1 Quantification of the difference in integrated signal level and the total difference in predicted apoptosis between DLD-N and the substituted data set

Signal	Substitution	Change in integrated signal	Change in total predicted apoptosis
pERK2	DKs8-N	420	−40
	DLD-1	520	−47
pHSP27	DKs8-N	22	3.2
	DLD-1	210	3.8
pIκBα	DKs8-N	7.9	−3.1
	DLD-1	−210	14
pJNK	DKs8-N	120	11
	DLD-1	340	23

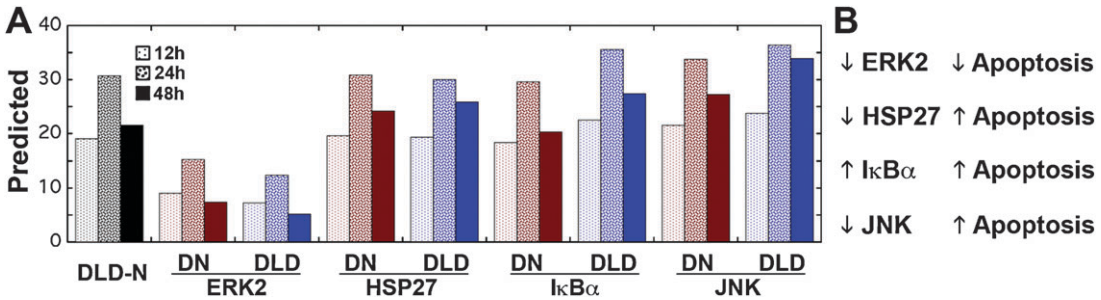

Fig. 4 **(A)** *In silico* predictions using mixed data sets demonstrate the balance between different signaling components. Apoptosis was predicted from the PLSR model using the full DLD-N signaling data set (black) *versus* data sets with three DLD-N time-courses and a single protein time-course substituted from DKs8-N (DN, red) or DLD-1 (DLD, blue). **(B)** Summary of the observed impact of changing signal data on the prediction of apoptosis.

dual-mutant cells heightened sensitivity to TNFα arises from increased pERK2 more than from enhanced pIκBα, inverting the relative contributions of these two pro-apoptotic signals compared to those in DLD-1 K-RAS mutant cells.

Discussion

Utilizing a multi-pathway model, we were able to predict the apoptotic response of a novel cell line expressing mutant forms of both K-RAS and N-RAS, which normally exert differential effects on the cellular response to TNFα. Following treatment with TNFα, DLD-N cells demonstrated activation of pERK2, pJNK, pHSP27, and pIκBα similar to N-RAS single mutant cells, while apoptosis was similar to K-RAS single mutant cells. Examination of the model demonstrated that the successful prediction resulted from the model interpretation of information from multiple pathways. Elevated pERK2 or pIκBα was interpreted by the model to correspond to increased apoptosis. After TNFα treatment, DLD-N exhibited the highest levels of pERK2 (which the model interpreted as more apoptosis) and pIκBα levels below DLD-1 (moderating the prediction of apoptosis). An analogous balance mechanism has been reported between signals involved in endocytosis and PI3K signaling in HER2 over-expressing mammary epithelial cells.[14] It is important to remember that PLSR models are correlative, and therefore, signals such as pIκBα and pERK2 that correlate to TNFα treatment may not be causative of apoptosis. In our previous studies of the single-mutant cell lines, experimental evidence suggested that pERK signaling that resulted from TNFα transactivation of TGFα had a net pro-death effect.[11]

Our motivation for this present work was to gain insights concerning how two mutations in the RAS pathway that exert opposite effects on apoptosis integrate to yield a cell fate decision. One potential effect would be for these mutations to exert additive or synergistic effects on another oncogenic pathway, for example proliferation or differentiation. However, our results indicate that with respect to TNFα-induced apoptosis, dual mutant cells phenocopy K-RAS mutant cells rather than showing a moderated level of apoptosis. Moreover, *in vivo* evidence does not support this interpretation for K-RAS and N-RAS. When expressed in the mouse colonic epithelium, mutationally activated K-Ras promotes proliferation, suppresses differentiation, and confers sensitivity to apoptotic stimuli.[3] Mutant N-Ras, by contrast, has no effect on proliferation or differentiation, but actively suppresses apoptosis.[3] One possible explanation for the co-existence of apparently contradictory mutations is that the mutations arise during circumstances of transient selective pressure. Currently available cancer genome sequencing data suggests that *KRAS* mutation is more effective at promoting sporadic colon cancer progression than is mutant *NRAS*—*KRAS* mutations occur in 30–40% of colon cancers, but *NRAS* mutations occur in only 3–5%. The rarity of N-RAS mutations suggests that they might arise under special selective pressure. Given the effect of activated N-RAS on the cellular response to TNFα, a pro-inflammatory cytokine, we suspect that *NRAS* mutations occur in cancers exposed to inflammation. Because of its deleterious effect with respect to apoptosis, *KRAS* mutation would likely not be advantageous during inflammation, and, indeed, *KRAS* mutations are less frequent in human colon cancers associated with chronic inflammation.[20] If the inflammation were transient, however, *NRAS* mutations might arise early during tumor progression, but then be expendable later in tumor progression because of regression of the inflammation. The loss of inflammation would set-up a permissive state for *KRAS* mutation. In essence, mutant N-RAS would allow the cancer to adapt to a transient selective pressure, but would later become a passenger mutation.

Conclusions

Integrative systems models such as the multi-pathway model of apoptosis presented here may provide a platform to identify key control mechanisms regulating cell behavior, resulting in novel drug targets. Our findings emphasize that signal-to-response relationships require multiple signaling pathways to be included in the model, as it is the balance of these signals that is interpreted by cells to make decisions.

Acknowledgements

We wish to acknowledge Roli Mandhana for her assistance in collecting lysate samples and members of the Lauffenburger lab for helpful discussions. We gratefully acknowledge Glenn Paradis of the Koch Institute Flow Cytometry Core Facility for technical assistance. This work was funded by National Institutes of Health Grants U54-CA112967 and P50-GM68762, and by the American Cancer Society (PF-08-026-01-CCG to P.K.K).

References

1 M. Malumbres and M. Barbacid, Ras. oncogenes: The first 30 years, *Nat. Rev. Cancer*, 2003, **3**, 459–465.
2 J. Downward, Targeting ras signalling pathways in cancer therapy, *Nat. Rev. Cancer*, 2003, **3**, 11–22.
3 K. M. Haigis, K. R. Kendall, Y. Wang, A. Cheung, M. C. Haigis, J. N. Glickman, M. Niwa-Kawakita, A. Sweet-Cordero, J. Sebolt-Leopold, K. M. Shannon, J. Settleman, M. Giovannini and T. Jacks, Differential effects of oncogenic k-ras and n-ras on proliferation, differentiation and tumor progression in the colon, *Nat. Genet.*, 2008, **40**, 600–608.
4 L. Klampfer, J. Huang, T. Sasazuki, S. Shirasawa and L. Augenlicht, Oncogenic ras promotes butyrate-induced apoptosis through inhibition of gelsolin expression, *J. Biol. Chem.*, 2004, **279**, 36680–36688.
5 J. C. Wolfman, T. Palmby, C. J. Der and A. Wolfman, Cellular n-ras promotes cell survival by downregulation of jun n-terminal protein kinase and p38, *Mol. Cell. Biol.*, 2002, **22**, 1589–1606.
6 K. Forrester, C. Almoguera, K. Han, W. E. Grizzle and M. Perucho, Detection of high incidence of k-ras oncogenes during human colon tumorigenesis, *Nature*, 1987, **327**, 298–303.
7 B. B. McConnell and V. W. Yang, The role of inflammation in the pathogenesis of colorectal cancer, *Curr. Colorectal Cancer Rep.*, 2009, **5**, 69–74.
8 J. Downward, Cancer: A tumour gene's fatal flaws, *Nature*, 2009, **462**, 44–45.
9 S. Shirasawa, M. Furuse, N. Yokoyama and T. Sasazuki, Altered growth of human colon cancer cell lines disrupted at activated ki-ras, *Science*, 1993, **260**, 85–88.
10 J. W. Keller, K. M. Haigis, J. L. Franklin, R. H. Whitehead, T. Jacks and R. J. Coffey, Oncogenic k-ras subverts the

antiapoptotic role of n-ras and alters modulation of the n-ras: Gelsolin complex, *Oncogene*, 2007, **26**, 3051–3059.
11 P. K. Kreeger, R. Mandhana, S. K. Alford, K. M. Haigis and D. A. Lauffenburger, Ras mutations affect tumor necrosis factor-induced apoptosis in colon carcinoma cells via erk-modulatory negative and positive feedback circuits along with non-erk pathway effects, *Cancer Res*., 2009, **69**, 8191–8199.
12 S. Gaudet, K. A. Janes, J. G. Albeck, E. A. Pace, D. A. Lauffenburger and P. K. Sorger, A compendium of signals and responses triggered by prodeath and prosurvival cytokines, *Mol. Cell. Proteomics*, 2005, **4**, 1569–1590.
13 K. A. Janes, S. Gaudet, J. G. Albeck, U. B. Nielsen, D. A. Lauffenburger and P. K. Sorger, The response of human epithelial cells to tnf involves an inducible autocrine cascade, *Cell*, 2006, **124**, 1225–1239.
14 N. Kumar, A. Wolf-Yadlin, F. M. White and D. A. Lauffenburger, Modeling her2 effects on cell behavior from mass spectrometry phosphotyrosine data, *PLoS Comput. Biol*., 2007, **3**, e4.
15 P. Geladi and B. R. Kowalski, Partial least-squares regression: A tutorial, *Anal. Chim. Acta*, 1986, **185**, 1–17.
16 L. Eriksson, E. Johansson, N. Kettaneh-Wold and S. Wold, *Multi- and megavariate data analysis: Principles and applications*, Umetrics, Umea, Sweden, 2001.
17 K. A. Janes, J. G. Albeck, S. Gaudet, P. K. Sorger, D. A. Lauffenburger and M. B. Yaffe, A systems model of signaling identifies a molecular basis set for cytokine-induced apoptosis, *Science*, 2005, **310**, 1646–1653.
18 D. Kumar, R. Srikanth, H. Ahlfors, R. Lahesmaa and K. V. Rao, Capturing cell-fate decisions from the molecular signatures of a receptor-dependent signalingresponse, *Mol. Syst. Biol*., 2007, **3**, 150.
19 B. D. Cosgrove, C. Cheng, J. R. Pritchard, D. B. Stolz, D. A. Lauffenburger and L. G. Griffith, An inducible autocrine cascade regulates rat hepatocyte proliferation and apoptosis responses to tumor necrosis factor-alpha, *Hepatology*, 2008, **48**, 276–288.
20 G. C. Burmer, D. S. Levine, B. G. Kulander, R. C. Haggitt, C. E. Rubin and P. S. Rabinovitch, C-ki-ras mutations in chronic ulcerative colitis and sporadic colon carcinoma, *Gastroenterology*, 1990, **99**, 416–420.

